



Optics Letters

Dynamically stable Nd:YAG resonators with beam quality beyond the birefringence limit and pumping of a singly resonant optical parametric oscillator

ALLAN BERCZKI, MÁRCIO ANDRÉ PRIETO APARÍCIO LOPEZ, AND NIKLAUS URSUS WETTER*

Centro de Lasers e Aplicações, IPEN-CNEN/SP, Av. Professor Lineu Prestes, 2242, São Paulo (SP), Brazil

*Corresponding author: nuwetter@ipen.br

Received 13 December 2017; revised 10 January 2018; accepted 10 January 2018; posted 10 January 2018 (Doc. ID 315539); published 7 February 2018

A simple, reliable, linearly polarized laser source with very high beam quality is demonstrated using standard diode-side-pumped Nd:YAG modules. The laser produced 30 W of output power with beam quality factor $M^2 < 1.15$ over the entire range of input powers and beam quality of 1.02 at the laser operation point. This is, to our knowledge, the highest beam quality for a dynamically stable high-power laser that uses an optically isotropic crystal. The laser was used as a pump source for an optical parametric oscillator based on a periodically poled lithium niobate, producing wavelength in the 1.5–3.8 μm range. © 2018 Optical Society of America

OCIS codes: (140.3410) Laser resonators; (140.0140) Lasers and laser optics; (140.3530) Lasers, neodymium; (140.3580) Lasers, solid-state; (140.3600) Lasers, tunable; (140.5560) Pumping.

<https://doi.org/10.1364/OL.43.000695>

Current laser systems are capable of delivering high-quality beams with high-power fiber lasers reaching several kW of output power while maintaining good beam quality [1–3]. Some of these commercially available systems can supply powers in the kilowatt range while maintaining near-diffraction-limited beam quality ($M^2 < 1.1$). Yet a simple, reliable, and cheap source for linearly polarized, high-quality beams remains of interest for a large number of applications, such as pump lasers for optical parametric oscillators (OPOs) and frequency conversion in general.

In this Letter, we demonstrate a simple and reliable laser source for high-quality beams with 30 W of linearly polarized output power and delineate the procedures to obtain such a beam quality. The laser was based on a previous work [4] in which we presented a Nd:YAG diode-pumped solid-state laser based on standard, commercial laser modules. Here, we improved the laser's beam quality in a controlled and calculated fashion to obtain a beam quality factor of 1.02 at the laser operation point. Furthermore, being a dynamically stable resonator,

it provided a continuous, linearly polarized 30 W of output power with a $M^2 < 1.15$ over the entire range of pump powers. A typical application for this range of output powers and beam quality is pumping of OPOs. The laser output was used to pump a singly resonant OPO cavity with a 40 mm periodically poled lithium niobate (PPLN) crystal, and wavelengths from 1500 nm to 3800 nm were produced, demonstrating a simple, low cost source for generation of tunable wavelengths in the range of 1500–3800 nm.

It is well known that every laser resonator containing a thermal lens has two stability zones [5]. Cerullo demonstrated that the stability zones can be joined, providing resonators with a wide dynamic range of operation, composed of both individual zones I and II [6]. This makes the use of joined stability zone resonators a good choice for working with laser cavities that are occupied by large fundamental TEM₀₀ modes (w_{30}) inside the laser rods, which is necessary for high output powers [7–9]. In such a case, both radial and tangential modes oscillate simultaneously, even though the width of a single stability interval is too small for both modes to oscillate simultaneously [4,10], given the limit for maximum beam waist size inside the rods (w_{30}^{BL}) imposed by thermally induced birefringent lensing:

$$(w_{30}^{\text{BL}})^2 \sim 3.5\lambda f, \quad (1)$$

where λ is the wavelength, and f is the average focal length of the thermal lens inside the rod at maximum pump power [11].

Equation (1) is derived from the fact that the difference between radial and tangential thermal induced lenses is approximately 20% for unpolarized lasers [11,12]. However, our experimental results demonstrate that for polarized lasers, the individual polarizations can depart strongly from this value, as will be shown in detail in this work. Our previous works have already shown that, depending upon the polarization, the values of radial and tangential thermal lenses can be almost the same [11]. Clearly, if the goal is beam quality, it is of interest to choose the polarization for which radial and tangential thermal lenses are as close as possible. In this way, the whole of the laser rod will experience a similar thermally induced refractive

gradient. If, on the contrary, the difference between the thermal lenses is large, one part of the beam will always be either multi-mode or unstable, generating a worse beam quality, which is clearly demonstrated by the much higher M^2 values [4,10].

Experimental setup. The laser employed a diode pumped laser module (HTOE Optoelectronics) containing a 78 mm long 0.6 at.% Nd-doped YAG rod pumped by twelve 808 nm diode bars arranged in a three-fold geometry. For the unpolarized laser, the measured thermal lens at 240 W of maximum pump power was $f = 18.2$ cm, corresponding to a birefringence-limited beam waist inside the rod of $823 \mu\text{m}$ [Eq. (1)]. The pump module's thermal lens was characterized as a function of pump power by combining a slit aperture and a polarizer as described in Ref. [11]. Shown in Fig. 1 is the difference of the measured radial and tangential dioptric powers in horizontal and vertical polarizations when compared to the mean value of the unpolarized resonator [Fig. 1(a)] and the ratio between radial and tangential focal lengths for vertical and horizontal polarizations [Fig. 1(b)].

The thermal lens components of the vertical polarization at the operation range above 190 W are much closer ($f_t/f_r \sim 1.11$) than for the horizontal polarization ($f_t/f_r \sim 1.25$). We therefore preferred the vertical polarization that allowed for closer values of the beam waist inside the rod in the radial and tangential directions.

It is important to observe that the choice of the vertical polarization does also allow higher w_{30} values; recalculating Eq. (1) with $f_t/f_r = 1.11$,

$$(w_{30}^{\text{BL}})^2 \sim 6.1\lambda f \quad (2)$$

results in a 32% bigger birefringence-limited stationary beam waist. For our pump module, it means that the stationary beam waist could be increased up to $1086 \mu\text{m}$. For a beam waist of that size, birefringence is no more the limiting factor, and diffraction effects at the rod aperture become dominant [12].

Next, the TEM₀₀ spot size inside the laser rod, w_{30} , as a function of rod dioptric power was simulated for different cavities and the corresponding misalignment sensitivity calculated, using a MATLAB code based on equations given in Refs. [5,13]. A convex–convex resonator, composed of two mirrors with radii $R_1 = -30$ cm and $R_2 = -50$ cm, was chosen

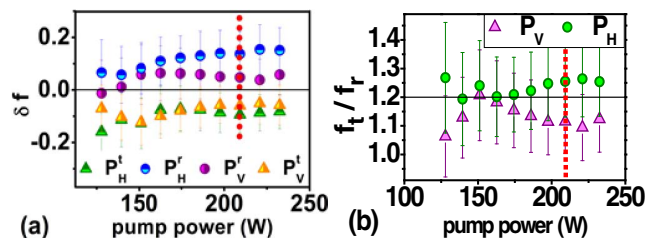


Fig. 1. (a) Normalized difference δf of rod polarized thermal lenses (measured in units of dioptric power) with unpolarized lens and ratio between measured tangential (f_t) and radial (f_r) focal lengths for horizontally P_H and vertically P_V polarized beams (b). Vertical dotted line is the laser operating point at 209 W of pump power. P_V and P_H denote beam polarized in the vertical and horizontal directions, respectively, while P^t and P^r denote radial and tangential polarizations, respectively. The values for the vertical polarization are closer together than for the horizontal polarization. Also shown (solid horizontal line) in (b) is the literature value of $f_t/f_r = 1.2$. Dotted vertical line is the operating point for $M^2 = 1.02$ in vertical polarization.

because it allows for large fundamental mode inside the rod while maintaining minimal sensitivity to misalignment along the stability interval [4]. The resonator was designed for joint stability zones, allowing the laser to accommodate both tangential and radial thermal lenses [6]. Output coupling was 30% ($R = 70\%$) at 1064 nm. Linear laser polarization was obtained by means of an intracavity thin-film polarizer, TFP (Layertec) designed for 45° incidence with $R_s > 99.8\%$ and $R_p < 1\%$.

In order to calculate the distances from the principal planes of the rod to the mirrors, L_1 and L_2 , we fixed the edge of the stability interval at maximum pump power corresponding to an average lens of 18.2 cm, which resulted in $L_1 = 35$ cm and $L_2 = 42$ cm. The distance between mirror 2 and TFP is 10 cm. The laser setup is shown in Fig. 2. Next, the resonator was shortened with concomitant decrements in distances L_1 and L_2 , observing the constraint of Fig. 3(a) and changing distance L_1 linearly with distance L_2 to keep the laser operation in joined stability zones. Shortening the resonator length becomes necessary because, as seen in Fig. 1(a), the vertical polarization has a smaller average focal length than the horizontal polarization. The final dimensions were $L_1 = 33.7$ cm and $L_2 = 41.6$ cm.

The effects of a length change on the resonator can be seen in Fig. 3(b): the lower stability limit at small pump powers (dashed line) varies slowly in terms of dioptric power (f^{-1}) as L_1 increases while the upper limit of stability zone I (dotted line) decreases faster, allowing us to choose how close the resonator should operate to the stability limit at maximum pump power.

On the other hand, the stability interval width in terms of dioptric power [difference between dotted and dashed lines; see

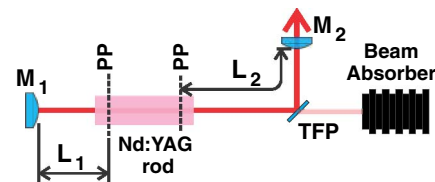


Fig. 2. Pump laser setup. PP, principal planes of rod; TFP, thin-film polarizer; M_1 , HR mirror; M_2 , output coupling mirror.

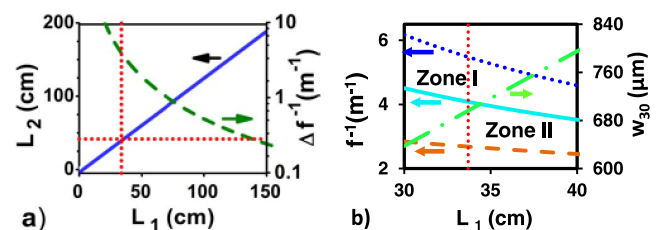


Fig. 3. (a) Calculated distances L_2 versus L_1 and corresponding widths of the stability interval (dashed line, right axis) for keeping joined stability zones using mirror radii $R_1 = -30$ cm and $R_2 = -50$ cm. Δf^{-1} is the dynamic range or width of the joined stability zones. (b) Calculated stability zones limits in terms of rod focusing power as distances L_1 and L_2 are changed, maintaining joined stability zones. Dotted curved line represents beginning of zone I; continuous line is transition between zone I and II, and dashed line is end of zone II; dashed–dotted line is corresponding stationary beam waist value w_{30} (right axis). Dotted horizontal and vertical lines represent final dimensions of resonator.

Fig. 3(b)] decreases with corresponding increase in stationary beam waist w_{30} . Both effects—the increase in stationary beam waist and the proximity to the border of the stability limit at maximum pump power (dotted line)—result in better beam quality. Therefore, this procedure makes it possible to fine-tune the point at which beam quality is maximum before the resonator becomes unstable.

At 209 W of pump power and average beam waist at the rod of 781 μm , with a corresponding thermal lens of 20.9 cm and tangential and radial values of the beam waist inside the rod differing by only 7%, the measured M^2 value was 1.02(2).

Figure 4 shows the stability diagram and the beam waist at the rod in the stability range. Clearly seen is [Fig. 4(b)] that if horizontal polarization were chosen, part of the laser beam (P_H^t) would operate outside the stability zone with a very large beam waist in the vertical direction, suffering strong diffraction effects, whereas the vertical polarization is contained neatly in the center of zone I.

Pumping of the singly resonant OPO. Figure 5 shows the singly resonant OPO (SROPO) setup. The pump laser passes through an optical isolator, a 2:1 expansion telescope, and is

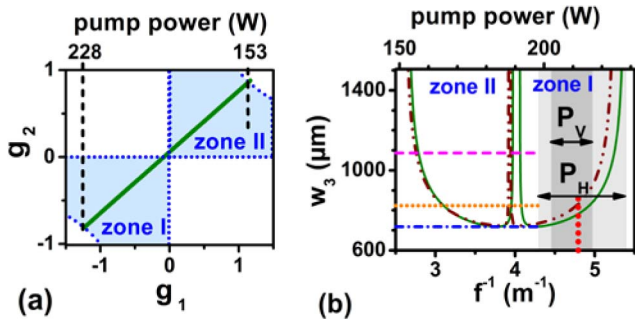


Fig. 4. (a) Stability diagram showing the dynamic range of operation from 153 W to 228 W of pump power (vertical dashed lines) and stability of resonator (solid diagonal line) as a function of pump power. (b) Beam waist in rod (w_3) as a function of pump power for the final resonator (continuous line) and for the original, non-polarized resonator (dashed–dotted–dotted line). Horizontal dashed–dotted line indicates w_{30} value. Horizontal dotted line represents the maximum birefringence limited stationary beam waist given by Eq. (1). Horizontal dashed line represents the maximum birefringence limited stationary beam waist given by Eq. (2). Vertical dotted line represents the pump power corresponding to the best-measured beam quality factor of 1.02 with the filled ranges indicating the difference between the radial and tangential focusing powers for horizontal (P_H) and vertical (P_V) polarizations in this condition.

then focused by a 75 mm lens into a concave–concave SROPO resonator. Half-wave plates were used before and after the optical isolator for adjusting power and angle of the polarization plane of the pump radiation focused into the OPO cavity. Mirror M_2 had partial reflection and was chosen to introduce further losses to the pump laser in order to limit the pump power to a maximum of 12 W. The OPO resonator consisted of a 40 mm long PPLN (Covesion Ltd.) with four 1 mm \times 1 mm periodically poled regions ranging from 29.52 μm to 31.59 μm between two mirrors with radii 50 mm. The beam waist in the center of the PPLN crystal was adjusted to 55 μm for both pump and resonant beams, resulting in a focusing parameter ξ of 1.1 for the pump and about 1.6 for the resonant beam ($\xi = L/(2z_r)$, where L is the crystal length, and z_r is the Rayleigh range). Both mirrors had reflectivity $R < 2\%$ at 1064 nm, $R > 99.9\%$ for 1410–1800 nm, and $R < 5\%$ for 3000–4000 nm.

Pump, idler, and residual signal beams exiting the resonator were separated by a prism prior to characterization. A spectrometer (NIRQuest 512–2.5 μm , OceanOptics) allowed detection of the signal beam spectrum as well as some spectral part of the idler beam. An additional spectrometer in the range of 670–1090 nm (HR2000, OceanOptics) also detected a residual second-harmonic generation of the signal beam, allowing a finer resolution in wavelengths. Beam quality of the OPO was characterized by the knife-edge method. Measurements were taken in both continuous-wave (cw) and pulsed conditions using a chopper, installed after the optical isolator, to obtain 500 μs pump pulses with 5% duty cycle.

Results. Pump power versus output power and beam quality factor, measured utilizing a slit scanning device (Beamscope P8, Dataray), are shown in Fig. 6 for the pump laser. Each point in the graph represents the average of three different measurement runs. Maximum output power was 30 W and best beam quality was $M^2 = 1.02(2)$, measured at 24.8 W of output power. The transition between stability zones is clearly seen at about 195 W of pump power. The M^2 value remained below 1.16 in the entire range of pump powers from 165 W to 235 W.

Maximum output power was lower than the 45 W from our previous work [4], this being a result from the choice of the vertical polarization, which has a smaller beam waist inside the rod at the same pump power. In order to operate with maximum output power at the birefringence limit given by Eq. (2), we would need mirrors with smaller negative radius of curvature, which were not available in the lab. However, the output power was still much more than the ~ 10 W of pump power needed for the OPO.

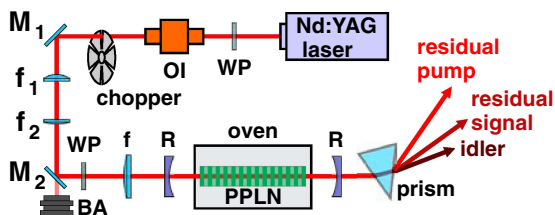


Fig. 5. Linear SROPO setup. WP, half-wave plate; OI, optical isolator; M_1 and M_2 , turning mirrors; f_1 and f_2 , 2:1 beam expander lenses; f , pump focusing lens; R, OPO cavity mirrors; BA, beam absorber.

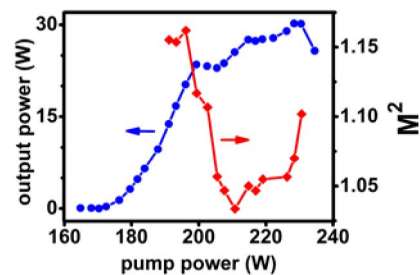


Fig. 6. Laser output power of pump laser (left axis) and corresponding beam quality factor (average of x and y directions; right axis).

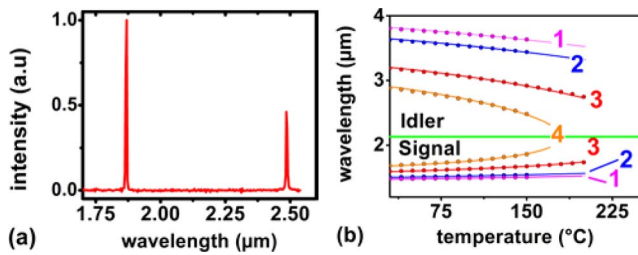


Fig. 7. (a) Output spectrum with $\Lambda_4 = 31.59 \mu\text{m}$ at 150°C showing both signal and idler beam peaks. (b) Measured wavelengths generated by the OPO and obtained with gratings 1–4.

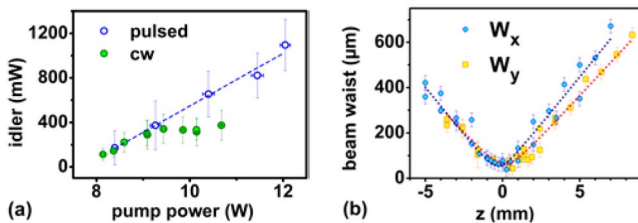


Fig. 8. (a) Idler beam output powers at 2486 nm ($\Lambda_0 = 31.59 \mu\text{m}$, 150°C) and (b) focused beam radius for beam quality measurement for idler at 2486 nm showing a $M^2 < 6$ value.

Figure 7(a) shows an output spectrum with grating $\Lambda_4 = 31.59 \mu\text{m}$ at 150°C where it is possible to identify both idler and signal beam peaks at $1.86 \mu\text{m}$ and $2.49 \mu\text{m}$, respectively. Figure 7(b) shows the wavelengths generated for crystal temperatures between 30° and 150° for the periodic gratings $\Lambda_1 = 29.52 \mu\text{m}$, $\Lambda_2 = 29.98 \mu\text{m}$, $\Lambda_3 = 31.02 \mu\text{m}$, and $\Lambda_4 = 31.59 \mu\text{m}$.

Figure 8 shows output power curves and knife-edge beam quality measurement for the idler beam with grating 4 at 150°C . For pulsed operation, 23.6% and 7.7% slopes were obtained for idler and signal beams, respectively, with 7.7 W threshold. For comparison, slightly better values have been reported in the literature [14,15], which might be due to back conversion affecting our OPO threshold and beam quality [16]. During cw operation [Fig. 8(a)], the behavior of the output power curve deviates from linear due to thermal effects in the crystal. For this reason, pump power in continuous mode was limited to avoid damage to the crystal. Measured M^2 values [Fig. 8(b)] were 5.7 and 5.8 in x and y directions, respectively.

Conclusion. We demonstrate that beam quality needs not be limited by thermally induced birefringence in dynamical stable resonators, even when using isotropic crystals such as YAG.

A beam quality of $M^2 = 1.02$ was obtained with a linearly polarized 1064 nm beam. The output remained stable in power and beam quality for several months without any realignment. The laser was built with standard, commercially available laser modules without any special sorting or conditioning. It is interesting to point out that the whole pump laser is a small fraction of the cost of an OPO crystal. Using this pump laser, a SROPO was successfully built, demonstrating its usefulness for such applications.

Funding. Fundação de Amparo à Pesquisa do Estado de São Paulo (FAPESP) (2006 53713-0, 2012 11437-8); Coordenação de Aperfeiçoamento de Pessoal de Nível Superior (CAPES) (COFECUB 710_11, 081_2013); Conselho Nacional de Desenvolvimento Científico e Tecnológico (CNPq) (2012_6 402241).

Acknowledgment. We would like to thank Prof. Malo Cadoret from CNAM for helpful discussions.

REFERENCES

1. Y. Jeong, J. K. Sahu, D. N. Payne, and J. Nilsson, *Opt. Express* **12**, 6088 (2004).
2. V. Gapontsev, V. Fomin, A. Ferin, and M. Abramov, *Lasers, Sources and Related Photonic Devices* (Optical Society of America, 2010), paper AWA1.
3. Y. Jeong, A. J. Boyland, J. K. Sahu, and S. Chung, *J. Opt. Soc. Korea* **13**, 416 (2009).
4. R. S. Pinto and N. U. Wetter, *Laser Phys.* **24**, 85801 (2014).
5. V. Magni, *Appl. Opt.* **25**, 107 (1986).
6. G. Cerullo, S. de Silvestri, V. Magni, and O. Svelto, *Opt. Quantum Electron.* **25**, 489 (1993).
7. N. U. Wetter, E. C. Sousa, F. D. A. Camargo, I. M. Ranieri, L. Sonia, F. de Almeida Camargo, I. M. Ranieri, and S. L. Baldochi, *J. Opt. A* **10**, 104013 (2008).
8. N. U. Wetter, F. A. Camargo, and E. C. Sousa, *J. Opt. A* **10**, 104012 (2008).
9. N. U. Wetter and A. M. Deana, *Opt. Express* **23**, 9379 (2015).
10. A. Berezcki and N. U. Wetter, *Opt. Laser Technol.* **96**, 271 (2017).
11. N. U. Wetter, E. P. Maldonado, and N. D. Vieira, *Appl. Opt.* **32**, 5280 (1993).
12. W. Koehner, *Solid-State Laser Engineering*, 6th ed. (Springer-Verlag, 2006).
13. S. de Silvestri, P. Laporta, and V. Magni, *Opt. Commun.* **59**, 43 (1986).
14. W. R. Bosenberg, A. Drobshoff, and J. I. Alexander, *Opt. Lett.* **21**, 713 (1996).
15. W. R. Bosenberg, A. Drobshoff, and J. I. Alexander, *Opt. Lett.* **21**, 1336 (1996).
16. L. Hui-Qing, G. Ai-Cong, B. Yong, P. Qin-Jun, C. Da-Fu, and X. Zu-Yan, *Chin. Phys. Lett.* **22**, 1694 (2005).